Regular Article

PHYSICAL CHEMISTRY RESEARCH
Published by the
Iranian Chemical Society
www.physchemres.org
info@physchemres.org

Phys. Chem. Res., Vol. 11, No. 4, 913-928, December 2023
DOI: 10.22036/pcr.2022.365510.2221

Elaboration and Characterization of Organo-Ghassoul (Moroccan Clay) as an Adsorbent Using Cationic Surfactant for Anionic Dye Adsorption

A. El Mahbouby[a], Y. Ezaier[b,*], I. Mechnou[a], Y. Raji[a] and S. Zyade[a]

[a]*Laboratory of Materials Engineering for the Environment and Valorization (LMEEV), Team (I3MP), Faculty of Sciences Aïn Chock, Hassan II University of Casablanca, Morocco*

[b]*Bio-Geosciences and Materials Engineering Laboratory, Higher Normal School, Hassan II University, Casablanca, Morocco*

(Received 17 October 2022, Accepted 7 December 2022)

This study used a cation-exchange method to carry out significant chemical modifications in Ghassoul (Moroccan clay) by inserting a cationic surfactant (N-methyl-N,N,N-trioctyl ammonium chloride) through the void between the leaves. The synthesized organophilic Ghassoul was characterized by Fourier transform infrared spectroscopy, X-ray fluorescence, X-ray diffraction, and thermogravimetric analysis. The experiments were conducted under static conditions to optimize certain parameters, such as the pH value, the adsorbent concentration, and the characteristic contact time. A variety of kinetic and equilibrium models were used to fit the data. The maximum adsorption capacity was 90%, with a mass-volume ratio of 0.6 g l^{-1} at pH = 5. The kinetic study revealed that the pseudo-second-order model was better suited for a contact time of about 60 min. The study of adsorption isotherms showed that the Langmuir model correctly described the adsorption process with an extreme adsorbed amount of up to 204 mg g^{-1} at 25 °C. Thermodynamic measurements revealed that the adsorption reaction was spontaneous and energetically exothermic. The organo-Ghassoul was also applied to synthetic wastewater samples and the results demonstrated that the solid had a good capability to treat anionic dye-contaminated wastewater.

Keywords: Adsorption, Kinetic study, Thermodynamic parameters, N-Methyl-N, N,N-trioctyl ammonium chloride

INTRODUCTION

Water is necessary for commerce and agriculture; thus, countries without proper access to it find it difficult to prosper economically. Therefore, having access to water is crucial for a country's development. In industrialized countries, it is not so much the quantity but the quality of the available water that is the problem [1]. Huge sums of money are spent each year to treat water to make it drinkable. After being used, one of the major environmental problems that need to be resolved is the accumulation of toxic and hazardous chemical pollutants, especially dyes from a variety of manufacturing processes, including those involved in textiles, food, paper, transportation, and pharmaceutical industries [3,4], in industrial effluents and their release into aquatic environments [2]. One of the biggest causes of water pollution is the textile sector, which uses a lot of water and produces a lot of colorful effluents, which are particularly soluble in water, are not properly treated before being dumped, and can reach watercourses used for human consumption [5]. One of the most popular dyes, used as a textile pigment, for coloring and printing acrylic textile fibers is Reactive Blue 19 (RB-19). This textile industry dye is teratogenic, mutagenic, and carcinogenic to living things. Additionally, it is poisonous to people, aquatic life, and microorganisms.

Ultrasound-assisted electrocoagulation [6], catalytic ozonation [7], electrochemical degradation [8], foam separation [9], and Fenton reaction [10] are common procedures for treating textile effluents. These processes are expensive and difficult to use, require specific installations,

*Corresponding author. E-mail: yassine.ezaier14@gmail.com

and consume more energy than adsorption treatments. Recently, the removal of these dyes by an adsorption mechanism on modified clays has become a feasible treatment solution because it is efficient, simple, and inexpensive. A variety of substances, including clays and zeolite adsorbents, can be employed to remove textile dyeing effluents from water [11].

In their natural state, clays have limited properties. As an example, their thermal instability, induced by the collapse of their structures due to dehydration at 100-200 °C, causes them to be supplanted by zeolites (apparent materials) [12]. Indeed, the surface adjustments of some clays of mineral sources have gained particular attention in recent years because they allow the implementation of innovative porous materials that may be involved in novel and cutting-edge technologies [13]. Organophilic treatment is used to give the clay greater adsorption toward organic compounds, leading to the development of organo-inorganic nanocomposites [14]. The resultant hybrid materials can then be utilized as efficient adsorbents of organic pollutants in water, soil, air, cosmetics, some rheological fluids, paints, refractory varnishes, *etc*. [15-16].

The clay used in the present study was extracted from the deposits of the Atlas Mountains, located in Morocco. It is used for facial and body treatments as well as hair treatments. Moroccan Ghassoul, a variety of magnesium smectite, is a 2:1 type clay mineral, the elemental sheet of which is composed of a layer of alumina between two layers of silica [17]. Smectites are characterized by an unstable structure that is reflected in their ability to swell in the presence of water and cations in interfoliar spaces [18]. The presence of cations in the interfoliar spaces is generated to compensate for the excess of negative charges on the octahedral layer. This can be explained by the isomorphic replacement of the ions Al^{3+} by Mg^{2+} ions, which are easily exchanged. In addition, the smectite platelets have a random shape, a very small size, an average diameter (0.1-1 μm), and a thickness varying between 1 and 10 nm [19]. Mineralogically, in addition to natural stevensite, which is the active substance of Ghassoul, a raw sample of Ghassoul may contain significant quantities of gypsum, calcium, and/or magnesium carbonates [20].

Several recent studies have been conducted on this Moroccan clay (Ghassoul) to develop new industrial applications. Twenty-eight articles were conducted between 1998 and 2016, of which twenty-four have focused on the practical application of Ghassoul [21]. Between 2016 and 2022, a similar number of articles were published on the application of Ghassoul as an adsorption unit. The majority of studies have reported that Ghassoul can be efficiently used as an adsorbent for cationic dyes and organic metals [22]. In 2022, Naboulsy *et al.* focused on the adsorption of two cationic dyes, including malachite green and Basic Yellow 28, with an adsorbed amount of 588 mg g^{-1} and 500 mg g^{-1}, respectively) [23]. Bouna *et al.* [24] reported a high removal efficiency of methylene blue (q_{max} = 240 mg g^{-1}) as compared to that of aqueous solutions. However, none of these studies have used Ghassoul to eliminate the anionic dye. In contrast, the removal efficiency of orange G (anionic dye) using natural Ghassoul was observed to be negligible. This difference can be explained by the attraction and repulsion forces between the negatively charged Ghassoul particles and the cationic and anionic dyes, respectively. Since anionic dyes are negatively charged, the clay surface should be treated with a suitable cationic surfactant to increase the effectiveness of their removal [25].

In this study, an N-methyl-N,N,N-trioctylammonium composite with high adsorption capacity was developed from Ghassoul using a method based on cation exchange. The developed organophilic Ghassoul was applied to the removal of RB-19 from water. The study aimed at addressing the following objectives: (i) detailed characterization of the developed organo-Ghassoul adsorbent (ii) detailed application of the developed organo-Ghassoul in the adsorption of RB-19 (the effects of initial pH, adsorbent dose, initial adsorbate concentration, contact time, temperature, isotherm, kinetics, and thermodynamics) (iii) interpretation of the adsorption mechanism.

MATERIALS AND METHODS

Purification of Ghassoul

The study sample of clay (Ghassoul) was taken from the Middle Eastern Atlas region of Morocco. The purification treatment adopted in this research was carried out as described in the literature [15]. The raw clay (GH-B) was first pulverized using a specific ceramic mortar and dehydrated at a temperature of 65 °C for 24 h to obtain fine powders sieved to 200 μm. Next, the sieved material was attacked by acetic

acid CH_3COOH and sodium acetate CH_3COONa buffer solution, and washed by hydrochloric acid HCl to decompose the carbonate CO_3^{2-}. Finally, the obtained material was washed several times with distilled water to remove both chloride ions Cl^- and ions formed by the reaction between impurities and acid [26].

Preparation of Homo-Ionic Ghassoul

Purified clay underwent a cationic exchange to replace different cations in the interfoliar space (Ca^{2+}, K^+ Mg^{2+}…) with the monovalent Na^+ ions, which facilitated the dispersion of the study clay into aqueous solutions. To achieve this objective, the sample was dispersed in a volume of 400 ml of a saturated sodium chloride solution under magnetic agitation for 12 h. After this procedure, the sample was washed again with sterile water to completely suppress the chloride and exchanged ions (negative silver nitrate $AgNO_3$ test) [27]. Finally, the homologized clay was dehydrated at 65 °C, crushed, and sifted at 200 µm. The purified Ghassoul was designated by GH-P. Table 1 provides the chemical mass composition of the brute and purified clay determined by X-ray fluorescence. The cationic exchange capacity (CEC) of the purified Ghassoul was measured using copper triethylenetetramine [28]. It is worth mentioning that the value found for CEC was estimated to be 48 meq/100 g of clay.

Preparation of Organoclays

The inorganic exchangeable cation (Na^+) is most frequently swapped out for an organic cationic surfactant to create organophilic clay [29]. A 10 g of GH-P was added to 400 ml of an N-methyl-N,N,N-trioctylammonium chloride $C_{25}H_{54}ClN$ solution at a concentration equivalent to the CEC. After 24 h of magnetic stirring at room temperature, the solid suspensions were centrifuged and washed several times with a certain mass of distilled water to remove all chloride ions ($AgNO_3$ test). Then, the suspensions were dried, crushed, and sieved to 200 µm. The organophilic synthesized clay was designated by (GH-M), as can be seen in Fig. 1, which summarizes the homoionization and modification processes.

Measurement and Characterization Method

Three characterization methods were employed to understand and ensure the purification and alteration of the clay used in this work. The samples were analyzed using a specific WDXRF spectrometer with a typical input power of 1 kW as the intensity of its X-ray generator. Furthermore, the X-ray diffraction configurations of the studied samples were

Table 1. Chemical Composition of GH-B and GH-P

Oxide / Sample	SiO_2	Al_2O_3	MgO	Na_2O	K_2O	CaO	Fe_2O_3
GH-B (%)	58.56	2.05	24.04	0.53	0.83	3.21	1.62
GH-P (%)	62.30	4.01	22.06	1.05	0.32	0.03	0.43

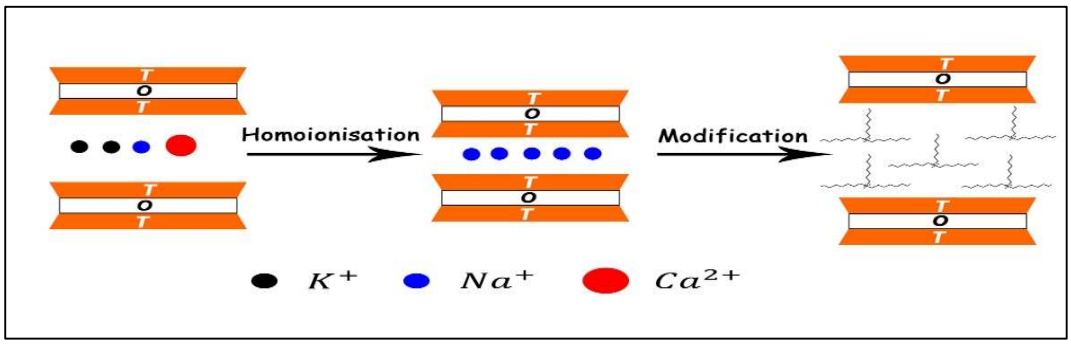

Fig. 1. Schematic representation of the process of modifying the clay layers by organic surfactant cations.

recorded using an advanced system known as Bruker D8, which provides a lower wavelength (~0.7 Å) than that of the emitted radiation from the copper source (~1.5 Å). The depiction by infrared spectroscopy (Jasco spectrophotometer-410) was recorded on a wavelength (ν = 1/λ) ranging from 400 cm^{-1} to 4000 cm^{-1}. Thermogravimetric analysis (TGA)/derivative thermogravimetry (DTG) analysis was conducted on a Cahn Versa Therm analyzer. The sample was heated in a corundum crucible from 30 to 1000 °C at a heating rate of 10 °C min^{-1} under air atmosphere (25 ml min^{-1}). Experimentally, the absorbance tests were made *via* a UV-Vis spectrophotometer (Shimadzu UV-2101PC) at a wavelength of λ_{max} = 594 nm for the incorporated reactive RB-19.

Kinetics and Adsorption Isotherms

The kinetic study of the adsorption of RB-19 on the GH-M was carried out under static conditions. The assembly comprised a thermostatic bath, in which a beaker containing the reaction mixture was immersed properly (colored solution C = 120 mg l^{-1}, adsorbent concentration m/v = 0.6 g l^{-1}) at the temperatures 25 °C, 35 °C, and 45 °C). All experiments were repeated three times to eliminate outliers. Following the stirring of the solution, the samples were involved at regular intervals while the remaining dye concentration was measured using UV-Vis spectroscopy. The pseudo-first/second order and intraparticle scattering approximations were all tested. The first-order approximation is governed by the following differential equation [30]:

$$\ln(q_e - q) = \ln(q_e) - K_1(T) \times t \quad (1)$$

Here, q and q_e are the amounts in (mol g^{-1}) adsorbed quantity at equilibrium and time t, respectively.

The second-order approximation is expressed analytically as follows [31]:

$$\frac{t}{q} = \frac{1}{K_2 \times q_e^2} + \frac{t}{q_e} \quad (2)$$

The intraparticle diffusion model is as follows [32]:

$$q = K_p \times t^{1/2} + c \quad (3)$$

Here, $K_1(\mathrm{min}^{-1})$, $K_2(\mathrm{g\,mg^{-1}\,min^{-1}})$, and $K_P(\mathrm{mg\,g^{-1}\,min^{-1/2}})$ are the kinetic constants characterizing the proposed models, respectively.

Several approximations have been proposed to describe the thermal feature of the adsorption phenomenon in aqueous media. In this work, the adsorption of RB-19 was made with an assembly comprising beakers containing reaction mixtures at different initial concentrations (120-240 mg l^{-1} by 20 mg l^{-1}) and a mass of 0.06 g GH-M. The whole was stirred for a time necessary to reach equilibrium. The adsorption results were modeled using Langmuir and Freundlich isotherms [33]. The linearized equations used for the models are as follows, respectively:

$$\frac{1}{q_e} = \frac{1}{q_{\max}} + \frac{1}{c_e \times K_L \times q_{\max}} \quad (4)$$

$$\ln(q_e) = \ln(K_f) + \frac{\ln(c_e)}{n} \quad (5)$$

where $Ce\ (\mathrm{mg}\ l^{-1})$ and $qe\ (\mathrm{mg}\ g^{-1})$: represent the concentration and the adsorbed quantity at the equilibrium, respectively, q_{max}: corresponds to the maximum value of the adsorption capacity, K_L is the physical constant of Langmuir, and K_F and n: are the physical constants of Freundlich.

The adsorbed quantity and the percentage of dye removal were calculated based on the following equations [34].

$$q_e = \frac{C_0 - C_e}{m} \times V \quad (6)$$

$$R(\%) = \frac{C_0 - C_e}{C_0} \times 100 \quad (7)$$

where $V\ (l)$ describes the volume taken for the solution, $C_0(\mathrm{mg\,l^{-1}})$ is the initial concentration of RB-19 in the liquid phase, and m (g) specifies the used mass of the adsorbent.

Thermodynamics Studies

To investigate the characteristics of the adsorption of RB-19 on GH-M, the standard free enthalpy ($\Delta G°$), the standard enthalpy ($\Delta H°$), and the standard entropy ($\Delta S°$) were calculated at the equilibrium for the resulting adsorption reaction. The partition coefficient (K_d) enabled us to

calculate all the above thermodynamic magnitudes based on the following equations [35]:

$$\Delta G^0 = -RT\ln(K_d) \quad (8)$$

$$\ln(K_d) = -\frac{\Delta H^0}{R\times T} + \frac{\Delta S^0}{R} \quad (9)$$

where $R\ (J\ mol^{-1}\ K^{-1})$ represents the molar gas constant and $T(K)$ denotes the absolute temperature.

RESULTS AND DISCUSSION

XRD Analysis

The findings for the analyzed clay samples are presented in Fig. 2. As can be seen in Figure 1, the XRD patterns of the Moroccan Ghassoul clay show the presence of diffraction peaks at 2θ = 20.23°, 30.43°, 33.40°, and 50.74°, indicating that the quantity of steven site was important in the Ghassoul fraction. The same XRD patterns also show the presence of an amount of quartz (Q) at 2θ = 22.73°, 26.72°, and 61.70°. The presence of free silica in the form of quartz and dolomite (D) at 2θ = 31.83°, 34.58°,45.03°, and 36.21° is also evident in very small amounts [35]. These findings are consistent with the XRD findings cited by other researchers [36-37].

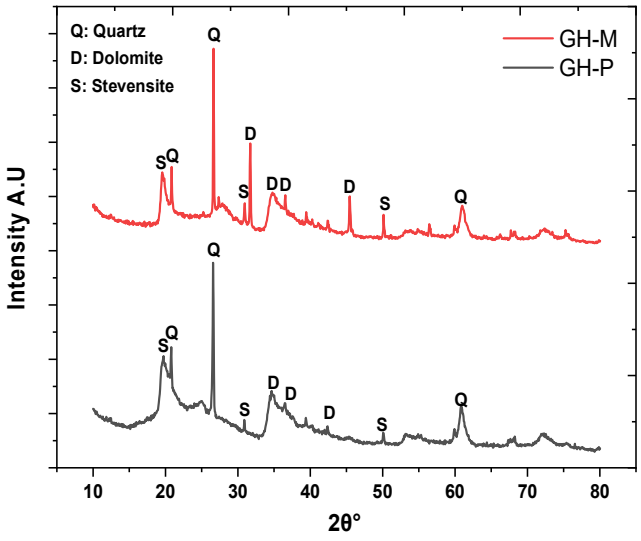

Fig. 2. The XRD patterns of purified clay (GH-P) and modified clay (GH-M).

XRF Analysis

The XRF results before and after the purification are shown in Table 1. The analysis of the results indicated that the principal constituents of the clay were silicon dioxide (SiO_2), aluminum oxide (Al_2O_3), magnesium oxide (MgO), and calcium oxide (CaO).SiO_2 and MgO contents of the raw clay were 58.56% and 24.04%, respectively. This particular structure of Ghassoul clay is due to the presence of trioctahedral magnesium smectite corresponding to stevensite. These findings agree with the XRD results reported in other studies [38]. It is important to note that sodium content increases while calcium and magnesium content decreases during the purification process. This is because sodium undergoes cationic exchange during sodium homoionization with sodium chloride solution and carbonate attack during acidification. Both of these processes (*i.e.*, cationic exchange and carbonate attack) increase sodium content.

Fourier Transform Infrared Spectroscopy (FTIR) Analysis

The FTIR findings of the GH-P and GH-M samples are illustrated in Fig. 3. The FTIR spectra of GH-P indicate a very broad and less intense band extending between 3000-4000 cm^{-1}, corresponding to the OH group vibrations [39]. The peaks at this band region were detected at 3613 cm^{-1} and 3709 cm^{-1}, due to the elongation vibrations of the octahedral layer OH group, of which the central metal was either Al or Mg [40]. The mode of vibration of the water molecule observed around 3400 cm^{-1} can be explained by the hydration of the sample. Another wide band with low intensity was detected around 1635 cm^{-1}, which can be attributed to the angular deformation vibrations of the water adsorbed in the interfoliar space [41]. A wide and intense band, located between 900-1200 cm^{-1} and centered about 985 cm^{-1}, corresponded to the stretching vibrations of Si-O-Si. The bands located at 450 cm^{-1} and 650 cm^{-1} can be attributed to Si-O-Mg. The analysis of the FTIR spectra also revealed that there was no band at 1400 cm^{-1}, which characterizes the valence vibration of the CO bond of the CO_3^2-group and provides some details on the purification performance [42]. The comparison of the two spectra obtained from GH-P and GH-M revealed some dissimilarities. For example, the new bands appeared around

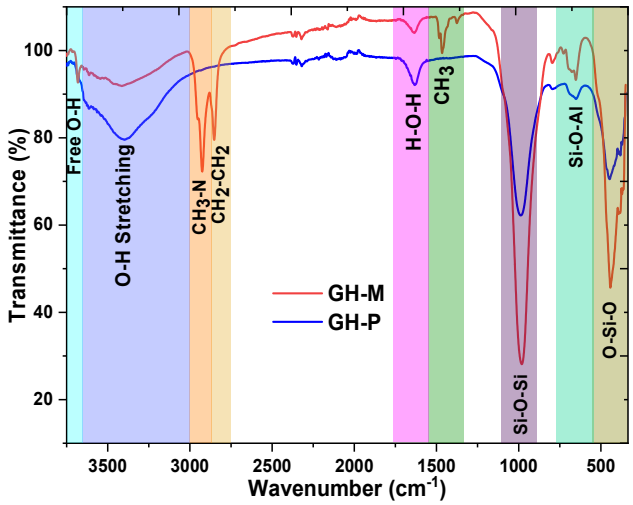

Fig. 3. The infrared spectra of purified clay (GH-P) and modified clay (GH-M).

2924 cm^{-1} and 2851 cm^{-1}, corresponding to the valence vibrations of the CH_3-N and -CH_2-CH_3 bonds, respectively, of which the latter are relative to organic molecules. The significant decrease of the bands at 3400 cm^{-1} and 1635 cm^{-1} can be justified by the effect of organic surfactants on the number of hydrated cations. The above results confirm the insertion of the N-methyl-N,N,N-trioctylammonium cation between the sheets of clay [43].

Thermogravimetric Analysis (TGA)

The content of surfactant in GH-M samples was calculated using the TG/DTG analysis. The TG curve of GH-P (Fig. 4) revealed two mass loss steps in the temperature ranges of 50-200 °C and 500-800 °C, corresponding with the associated DTG peaks located at 88 °C and 780 °C, respectively. The first loss step was 10%, which was located within the temperature range of 50-200 °C and corresponded to the loss of mass linked to the departure of water molecules of the interfoliar space. This significant weight loss reflects the swelling nature of the GH-M and the strong hydration of interfoliar cations. That is described as a specific swelling behavior of smectites. The second weight loss was 8%. It occurred for temperatures above 600 °C and corresponded to the dehydroxylation of steven site. The total loss is estimated at 20%. This result is in accordance with that of Bentahar *et al*. [45]. The temperature and amount of free water both decreased significantly as a result of the shift in the surface affinity (from hydrophobicity to hydrophilicity) of the clay treated with a surfactant, as seen in the TG-DTG curves of GH-M (Fig. 5). Mass loss was also observed for the GH-P in the temperature range of 156-456 °C. Evaporation/decomposition of N-methyl-N,N,N-trioctylammonium cations from GH-M must have caused mass losses because GH-P is thermally stable in the above-mentioned temperature range [46]. The total loss is estimated at 31.32%.

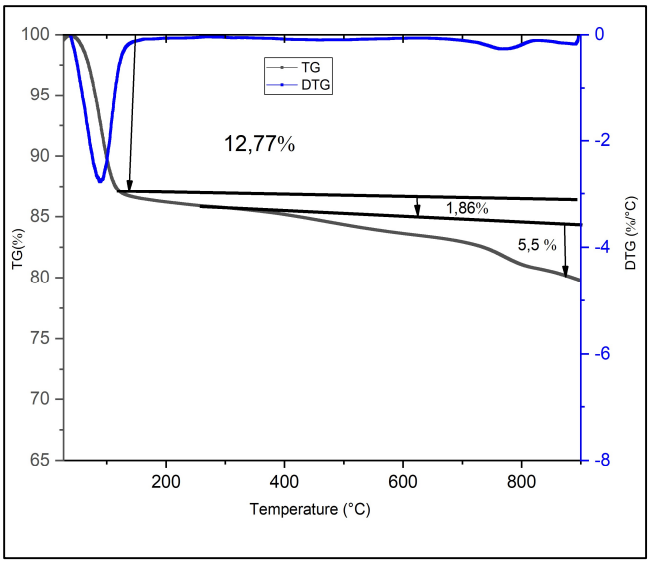

Fig. 4. The TG and DTG curves of the purified clay (GH-P).

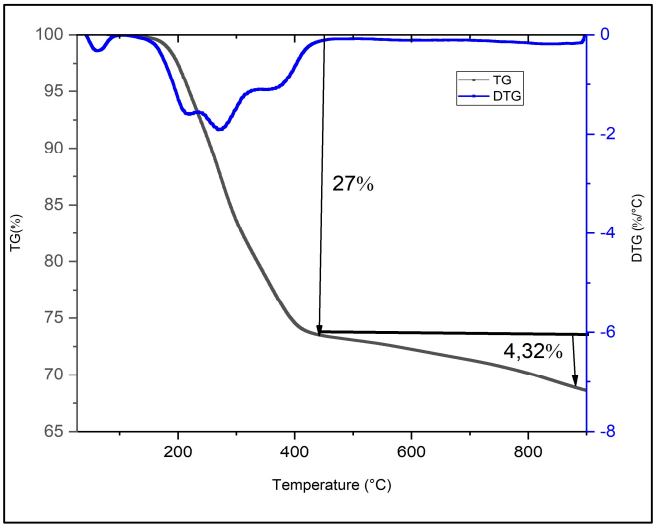

Fig. 5. The TG and DTG curves of the modified clay (GH-M).

Removal of Reactive Blue 19 (RB-19) via Adsorption onto the Modified Ghassoul

Adsorption studies. Effect of initial pH: The pH value of the solution had a significant effect on the adsorption process. Furthermore, it was found to significantly affect the effective surface charge, the crystal structure of the adsorbents, and the molecular structures of adsorbents. The pH effect of the RB-19 adsorption on the GH-M was evidenced under the following conditions:

-The initial value of the concentration C_0 is 120 mg l^{-1};

-The optimum dose of the adsorbent is 0.6 g l^{-1};

-The ambient temperature is 25 °C;

-The contact time is 60 min.

-The range of the initial pH value of the analyzed solution was boosted from 4 to 8. Figure 6 represents the performance of the adsorbent GH-M over the studied temperature range. The higher value found for the adsorption capacity at acid pH values was due to the surface of the adsorbent, which was protonated and positively charged. This increased the electrostatic attractive forces between the anion $-SO_3^-$ of the dye RB-19 and the adsorbent surface, which, in turn, enhanced the electrostatic attraction between this anion and the head of the surfactant due to its positive charge [47]. The maximum removal percentage took place at pH = 5, a value which can be suggested for future experiments.

Chemical Influence of the Adsorbent Concentration

To evaluate the extractive capacity of the GH-M concerning RB-19, we examined the effect of the support mass on the discoloration at 100 ml solution volume and 120 mg l^{-1} RB-19 concentration. The range of the adsorbent dose varied from 0.3 to 1 g l^{-1}. Figure 7 shows the effect of the adsorbent concentration on the RB-19 removal. It was observed that the adsorption efficiency increased with the support mass. This finding can be explained by the growth in the effective sites that continued until it reached its maximum value m = 0.6 g l^{-1} for the adsorbent dose, which can subsequently be used in future experiments.

The Effect of the Initial Dye Concentration

The influence of the initial dye concentration is displayed in Fig. 8. Generally, the RB-19 removal percentage decreased as the initial dye concentration was increased. This finding is principally due to the adsorption site saturation on the effective adsorbent surface [48], in which there are unoccupied accessible sites on the adsorbent surface at low concentrations. The necessary active sites for the microscopic adsorption of dye molecules disappeared quickly as the initial dye concentration was increased. However, the increase in the initial dye concentration

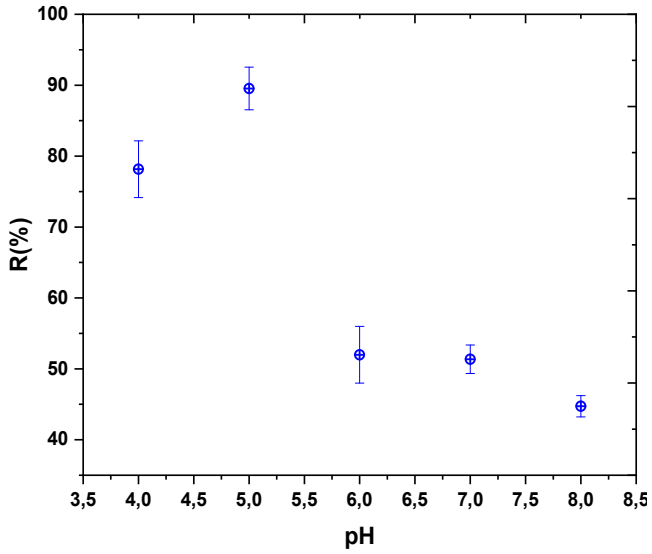

Fig. 6. The effect of pH on the adsorption of RB-19 onto the modified clay (GH-M) (initial concentration = 120 mg l^{-1}, adsorbent dose = 0.6 g l^{-1}, temperature = 25 °C).

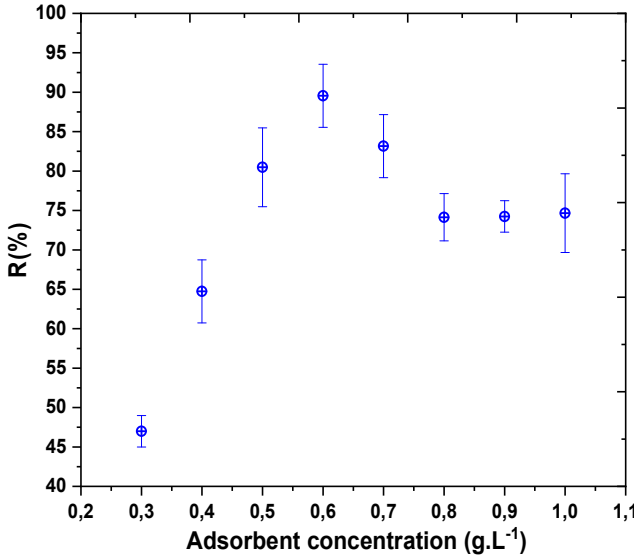

Fig. 7. The effect of adsorbent dose on the adsorption of RB-19 onto the modified clay (GH-M) (initial concentration = 120 mg l^{-1}, pH = 5, temperature = 25 °C).

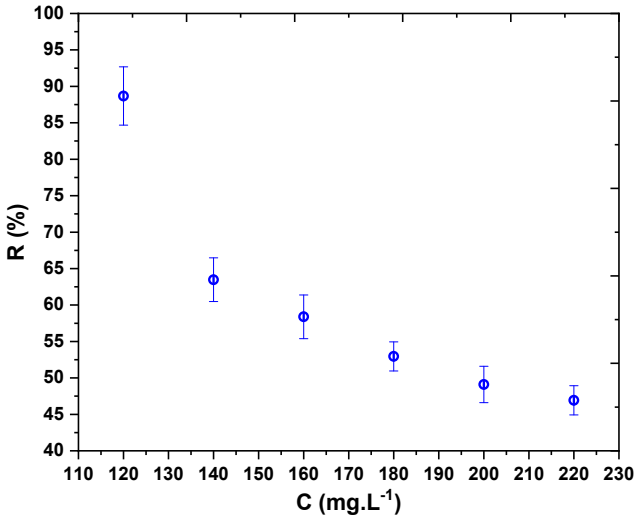

Fig. 8. The effect of initial concentration on the adsorption of RB-19 onto the modified clay (GH-M) (pH = 5, adsorbent dose = 0.6 g l^{-1}, temperature = 25 °C).

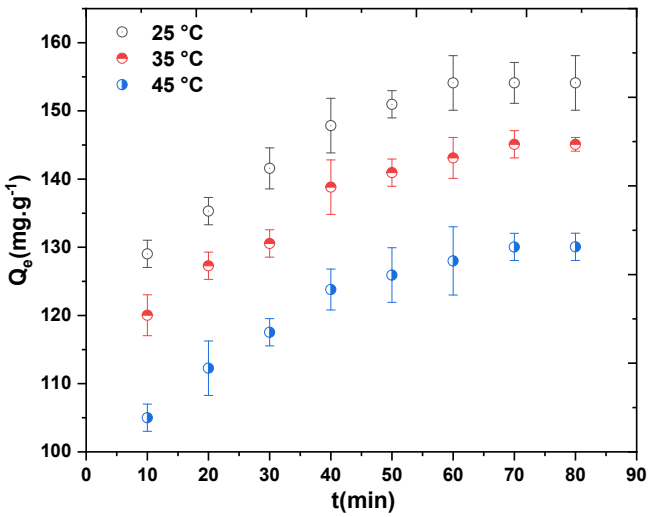

Fig. 9. The effect of the contact time on the adsorption of RB19 onto the modified clay (GH-M) at various temperatures (initial concentration = 120 mg l^{-1}, adsorbent dose = 0.6 g l^{-1}, pH = 5).

increased the adsorbent loading potential, which can be attributed to the higher driving force at higher initial dye concentrations. At increased initial dye concentrations, the remaining concentration of dye molecules had higher values. In the case of lower dye concentrations, the ratio between the initial quantity of dye molecules and the existing adsorption sites was weak. Thus, the fractional adsorption process became independent of the initial dye concentration [49].

The Effect of Contact Time and Temperature

The temporal evolution of the adsorbed amount of RB-19 on GH-M at different thermal conditions (25 °C, 35 °C, and 45 °C) is shown in Fig. 9, where $C_0 = 120$ mg l^{-1} for the RB-19 and $m = 0.6$ g l^{-1} for the GH-M. The shape of the kinetic curves at each temperature made it possible to define two zones. The first part of the curve revealed rapid adsorption, corresponding to the adsorption of the RB-19 on most quickly accessible sites, probably located on the peripheral surfaces of the material particles and the edges of the sheets [50]. The second part was in the plateau, form where the solute adsorption was maximum.

The adsorption kinetics became relatively slower at this level. This limitation of the adsorption rate is probably due to the molecular diffusion of the RB-19 in less accessible sites, such as the galleries of the interfoliar space [51]. In particular, the partition of a molecule between the liquid and solid phases depends on its water solubility, which is a function of its hydrophobic or hydrophilic nature linked to its chemical structure [52]. In general, the more soluble the organic molecules in the aqueous process are, the less adsorbent they will appear to be. It should be noted that for many organic molecules, water solubility tends to increase with temperature [53]. This probably explains the increase in the adsorbed amount with the thermal enhancement at the equilibrium state, which, in turn, weakens the attraction between the clay and RB-19. This decrease also indicates that the effect of the adsorption of the RB19 on the GH-M was controlled by a process of exothermic and physical adsorption.

Adsorption Kinetics

To understand the effect of the GH-M on RB-19 and analyze the adsorption mechanism, three kinetic models, namely, pseudo-first-order, pseudo-second-order, and intraparticle diffusion models, were adopted and represented by the linear forms of Eqs. (1), (2) and (3). Figures 10, 11, and 12 illustrate the plots of these equations.

Table 2 lists the adsorption rate constant values (K1 and K2) and the measured adsorption capacities values at

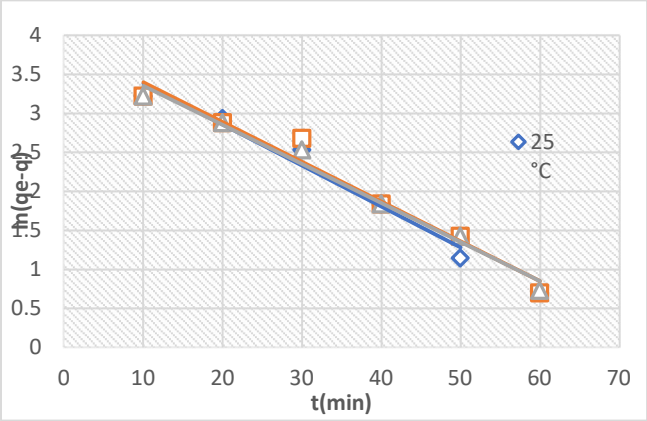

Fig. 10. The linear pseudo-first-order model of the adsorption of RB-19 on the GH-M.

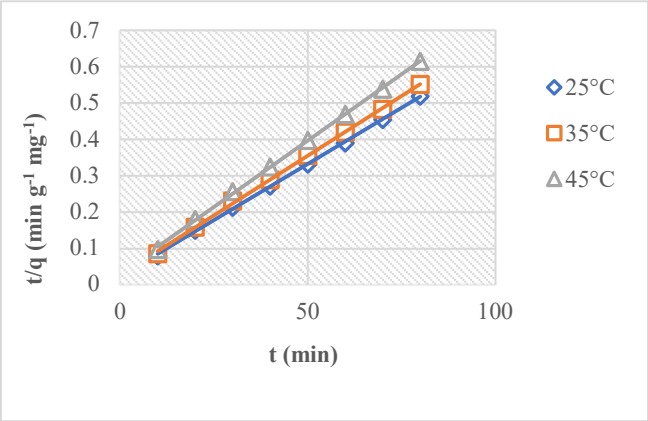

Fig. 11. The linear pseudo-second-order model of the adsorption of RB-19 on the GH-M.

equilibrium (q_e). Based on the results, it can be stated that in the case of first-order kinetics, the experimentally determined quantities adsorbed at the equilibrium were different from those calculated by the theoretical model. On the other hand, for the second-order kinetics, the quantities adsorbed experimentally were closer to those calculated using the theoretical model. Furthermore, the R2 values were very high and exceeded those obtained with the pseudo-first-order model, which confirms that the adsorption mechanism can be featured by the pseudo-second-order model. Early adsorption was due to surface adsorption. When the adsorption sites on the surface had reached saturation, RB-19 began to enter the

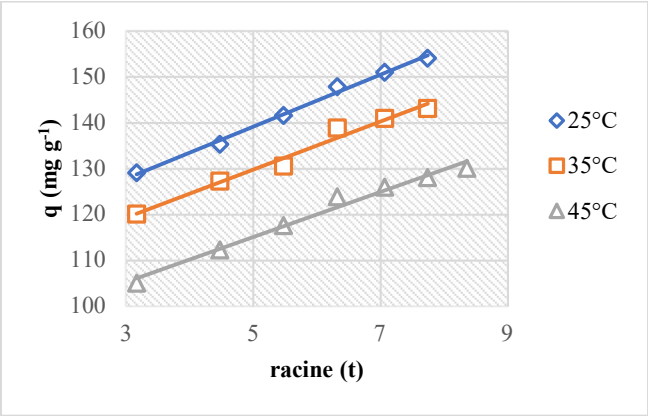

Fig. 12. The linear representation of the RB19 adsorption intraparticle diffusion on the GH-M.

Table 2. Kinetic Parameters of RB19 Adsorption on the GH-M

		25 °C	35 °C	45 °C
First-order kinetic model	K_1 (min^{-1})	0.0526	0.051	0.0501
	q_e (mg g^{-1})	49.8640	49.7594	47.2664
	R^2	0.9683	0.9682	0.9845
Second-order kinetic model	K_2 (g mg^{-1} min^{-1})	0.001848	0.001925	0.001925
	q_e (mg g^{-1})	161.2900	147.0588	136.9863
	R^2	0.9995	0.9993	0.9995
Intraparticular diffusion	K_p (mg (g $min^{0.5})^{-1}$)	4.194	4.9819	4.9125
	C (mg g^{-1})	110.81	104.79	90.462
	R^2	0.9816	0.9785	0.9816
q_e (mg g^{-1})		154.10	145.10	130.07

adsorbed pores and adsorbed onto the inner walls. The slow diffusion of RB-19 into the pores was confirmed by the low K value [54].

Isotherms and Thermodynamic Adsorption Parameters of RB-19

The adsorption of the dye RB-19 by the GH-M allowed us to determine the adsorption capacity and mechanism as well as the proposed design systems [55]. In this respect, the results of the adsorption process were modeled based on the Langmuir (Fig. 13) and Freundlich (Fig. 14) isotherms. Equations (4) and (5) were used to develop the models. Table 3 gives the parameters for each model. The application of Langmuir and Freundlich isotherms to the experimental points indicated that the Langmuir model was the best approximation for describing the removal of RB-19 via adsorption onto the GH-M since its coefficient of determination was higher than that of the other model. The value of the Freundlich constant n gives information on the degree of deviation of adsorption compared to the linearity. If n is equal to 1, absorption is linear, and if n is greater than 1, it implies that the adsorption process is physical, but if n is less than 1, it means that the adsorption process is chemical. Based on the results shown in Table 3, all n values were greater than unity, which confirms that the GH-M adsorption mechanism for RB19 was physical. The increase in the n value with the decrease in the temperature confirms that the adsorption was preferred at low temperatures, which can be explained by the weakening of physisorption and electrostatic interaction between RB-19 and the GH-M.

In Table 4, the q_{max} of the GH-M is compared to the adsorption capacities of other adsorbents used for RB-19 dye adsorption. This comparison shows that GH-M is a promising and effective adsorbent for removing textile-reactive dyes, such as RB-19, from the aqueous environment.

The thermodynamic quantities ($\Delta H°$ and $\Delta S°$) related to the study adsorption were derived from the slope parameter and the interception of the curve $ln(K_d)$, as a function of $1/T$ of Eq. (8) (Fig. 15) whereas the value of ($\Delta G°$) was estimated using Eq. (7). Table 5 presents the results.

The value of $\Delta G°$ for changing temperatures took negative values, suggesting that the GH-M removal cycle was spontaneous in solution [56]. The calculated values of

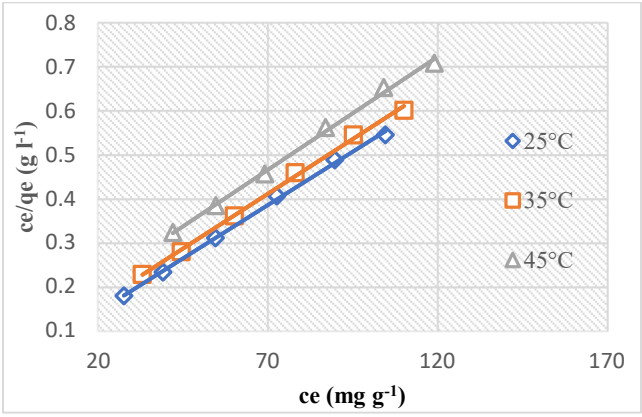

Fig. 13. Schematic representation of the adsorption of Langmuir isotherm.

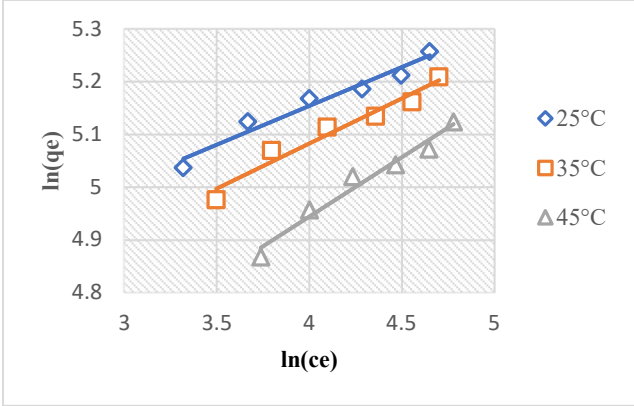

Fig. 14. Schematic representation of the adsorption of Freundlich isotherm.

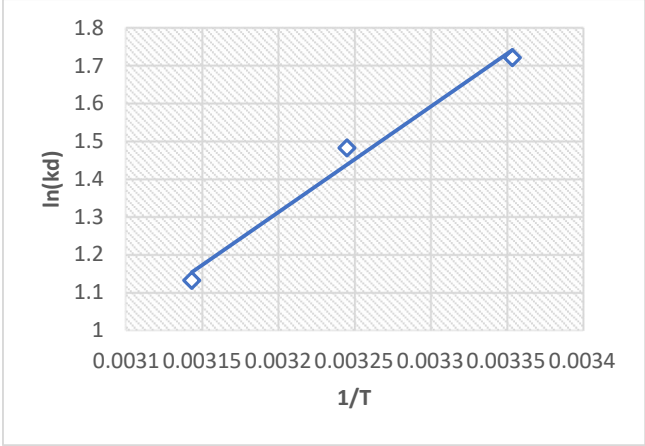

Fig. 15. The evolution of the logarithm of the thermodynamic constant according to 1/T.

Table 3. RB-19 Adsorption on GH-M with Langmuir and Freundlich Isotherms

Model	Temperature (°C)		
	25 °C	35 °C	45 °C
Langmuir			
q_{max} (mg g^{-1})	204.0816	200	192.3076
K_L (l mg^{-1})	0.1056	0.0794	0.0490
R^2	0.9981	0.9977	0.9972
Freundlich			
K_F	96.106	81.3857	57.1283
n	7.0077	5.8513	4.4503
R^2	0.9583	0.9539	0.9672

Table 4. A Comparison of the Adsorption Capabilities of RB-19 Dye by Various Adsorbents

Adsorbents	Q_{max} (mg g^{-1})	Ref.
Bentonite DTMA	206.85	[61]
DAH-bentonite	124.82	[62]
NiO-nanoparticles	98.83	[63]
MgO-nanoparticles	166.6	[64]
Paper sludge acitivated carbon	158	[65]
Furnace slag	74.7	[66]
Ghassoul-modified	204	This study

Table 5. Thermodynamic Parameters

ΔH°	ΔS°	ΔG° (kJ mol^{-1})		
(kJ mol^{-1})	(J mol^{-1} K^{-1})	25 °C	35 °C	45 °C
-23.2293	-63.4241804	-4.2684	-3.7987	-2.9926

enthalpy at different temperatures were also less than zero, showing that the process was energetically exothermic [57]. The negative value of $\Delta S°$ indicates that no change occurred in the internal structure of GH-M during the adsorption and that there was a reduction in disorder in the solid/solution interface throughout the adsorption operation [58]. The interval of $\Delta G°$ for the physisorption was generally between -20 kJ mol^{-1} and 0 kJ mol^{-1}, which confirms the thermo-kinetics results of the adsorption procedure [59]. The increase in the value of ΔG° with the increase in the temperature indicates that the heating process was adversely affected by RB-19 adsorption onto the GH-M [60].

The Proposed Adsorption Mechanism of RB-19

The chemical composition of Ghassoul changes from hydrophilic to hydrophobic due to the intercalation of N-methyl-N,N,N-trioctylammonium *via* ion exchange with inorganic cations. The cationic surfactant (N-methyl-N,N,N-trioctylammonium) adsorption mechanism on the negative surface of Ghassoul is identical to that of RB19 molecules on the positive surface of organophilic Ghassoul. In this study, the electrostatic force between the participating particles was found to be the governing mechanism of adsorption. In aqueous solution, the surfactant was hydrolyzed, and the dissociating effect of water intervened, negating its role as an acid. An amphiphilic compound was then formed: It had a polar pole (quaternary ammonium), which established bonds with water, and an apolar phase, which had affinity for apolar compounds. The hydrophilic head of the surfactant was attached to the aluminosilicate surface of Ghassoul. In fact, when the surfactant molecule entered the Ghassoul shell space, the electrostatic attraction generated between the Ghassoul alkyl chains and the N^+ cation led to a strong bond between them [67]. The electrostatic interaction between the anionic sections of the dye structure (SO_3^-) and the high positive surface of the organophilic Moroccan clay explain the RB-19 adsorption mechanism onto the GH-M. This process led to ultrahigh adsorption capacities of the GH-M for the RB-19.

CONCLUSIONS

In this work, the Moroccan clay (Ghassoul) was purified and given an organophilic character by inserting trimethyl ammonium chloride between its leaves, leading to the expansion of the spaces between the leaves and thus making them conducive to the adsorption and retention of various types of harmful organic pollutants released by different industrial activities. The success of the purification of the

GH-P was confirmed by the chemical analysis of the raw and GH-P using X-ray fluorescence and FTIR. The success of the modification was proven by three physicochemical techniques, namely, FTIR spectroscopy, XRF analysis, and TGA. The adsorption of RB-19 by organo-Ghassoul was carried out. The results of the kinetic and thermodynamic studies showed that this phenomenon was spontaneous, exothermic, and favored by a drop in temperature. The lines obtained for the considered models agreed with the experimental equilibrium results for three temperatures. However, when the statistical coefficient R^2 was greater than 0.99, Langmuir isotherm offered a better harmony compared to that of Freundlich. The modeling of the adsorption kinetics proved its validity with the pseudo-second-order model. According to the intraparticle diffusion model, the coefficient of determination was not neglected, showing the presence of an involved diffusive process for this system. In summary, it can be concluded that creating organophilic clay from an abundant Moroccan substance, called Ghassoul, is a creative and promising method for removing anionic organic compounds. Future studies should focus on the reusability, cost, and effect of activation methods prior to organic modification on the removal efficiency of clay-based adsorbents in practical wastewater treatment.

REFERENCES

[1] Campbell, T. A.; Booth, E. G.; Gratton, C.; Jackson, R. D.; Kucharik, C. J., Agricultural Landscape Transformation Needed to Meet Water Quality Goals in the Yahara River Watershed of Southern Wisconsin. *Ecosystems*., **2022**, *25*, 507-525, DOI: 10.1007/s10021-021-00668-y.

[2] Ihekweme, G. O.; Shondo, J. N.; Orisekeh, K. I.; Kalu-Uka, G. M.; Nwuzor, I. C.; Onwualu, A. P., Characterization of Certain Nigerian Clay Minerals for Water Purification and Other Industrial Applications. *Heliyon*., **2020**, *6*, e03783, DOI: 10.1016/j.heliyon.2020.e03783.

[3] Athar, M.; Imdad, S.; Zaidi, S.; Yusuf, M.; Kamyab, H.; Jaromír Klemeš, J.; Chelliapan, S., Biodiesel Production by Single-Step Acid-Catalysed Transesterification of Jatropha Oil under Microwave Heating with Modelling and Optimisation Using Response Surface Methodology., *Fuel*, **2022**, *322*, DOI: 10.1016/j.fuel.2022.124205.

[4] Nyankson, E.; Kumar, R. V., Removal of Water-Soluble Dyes and Pharmaceutical Wastes by Combining the Photocatalytic Properties of Ag_3PO_4 with the Adsorption Properties of Halloysite Nanotubes. *Mater. Today, Adv*., **2019**, *4*, 100025, DOI: 10.1016/j.mtadv.2019.100025.

[5] Martinez Stagnaro, S. Y.; Volzone, C., Adsorption of Anionic Dyes Monoazo and Diazo Using Organo-Bentonites., SN *Appl., Sci*., **2019**, *1*, 1-10, DOI: 10.1007/s42452-018-0070-3.

[6] Özyonar, F.; Gökkuş, Ö.; Sabuni, M., Removal of Disperse and Reactive Dyes from Aqueous Solutions Using Ultrasound-Assisted Electrocoagulation., *Chemosphere*., **2020**, *258*, DOI: 10.1016/j.chemosphere.2020.127325.

[7] Hu, E.; Shang, S.; Chiu, A. K. L., Removal of Reactive Dyes in Textile Effluents by Catalytic Ozonation Pursuing On-Site Effluent Recycling. *Molecules*., **2019**, *24*, DOI: 10.3390/molecules24152755.

[8] Santos, D. H. S.; Duarte, J. L. S.; Tavares, M. G. R.; Tavares, M. G.; Friedrich, L. C.; Meili, L.; Pimentel, W. R. O.; Tonholo, J.; Zanta, C. L. P. S., Electrochemical Degradation and Toxicity Evaluation of Reactive Dyes Mixture and Real Textile Effluent over DSA® Electrodes. *Chem. Eng. Process. Process Intensif*., **2020**, *153*, 107940, DOI: 10.1016/j.cep.2020.107940.

[9] Soylu, M.; Gökkuş, Ö.; Özyonar, F., Foam Separation for Effective Removal of Disperse and Reactive Dyes from Aqueous Solutions. *Sep. Purif. Technol*., **2020**, *247*, DOI: 10.1016/j.seppur.2020.116985.

[10] Tavares, M. G. R.; Santos, D. H. S.; Tavares, M. G.; Duarte, J. L. S.; Meili, L.; Pimentel, W. R. O.; Tonholo, J.; Zanta, C. L. P. S., Removal of Reactive Dyes from Aqueous Solution by Fenton Reaction: Kinetic Study and Phytotoxicity Tests. Water. Air. *Soil Pollut*., **2020**, *231*, DOI: 10.1007/s11270-020-4465-6.

[11] Mahmoodi, N. M.; Taghizadeh, A.; Taghizadeh, M.; Azimi, M., Surface Modified Montmorillonite with Cationic Surfactants: Preparation, Characterization, and Dye Adsorption from Aqueous Solution. *J. Environ. Chem. Eng.,* **2019**, *7*, 103243, DOI: 10.1016/j.jece.2019.103243.

[12] Halalsheh, N.; Alshboul, O.; Shehadeh, A.; Al Mamlook, R. E.; Al-Othman, A.; Tawalbeh, M.; Saeed Almuflih, A.; Papelis, C., Breakthrough Curves Prediction of Selenite Adsorption on Chemically Modified Zeolite Using Boosted Decision Tree Algorithms for Water Treatment Applications., *Water (Switzerland)*., **2022**, *14*, DOI: 10.3390/ w14162519.

[13] Zhang, S.; Liu, Q.; Cheng, H.; Gao, F.; Liu, C.; Teppen, B. J., Thermodynamic Mechanism and Interfacial Structure of Kaolinite Intercalation and Surface Modification by Alkane Surfactants with Neutral and Ionic Head Groups. *J. Phys. Chem*., **2017**, *121*, 8824-8831, DOI: 10.1021/acs.jpcc.6b12919.

[14] Xie, J.; Wang, Z.; Zhao, Q.; Yang, Y.; Xu, J.; Waterhouse, G. I. N.; Zhang, K.; Li, S.; Jin, P.; Jin, G., Scale-Up Fabrication of Biodegradable Poly(Butylene Adipate-Co-Terephthalate)/Organophilic-Clay Nanocomposite Films for Potential Packaging Applications. *ACS Omega*., **2018**, *3*, 1187-1196, DOI: 10.1021/acsomega.7b02062.

[15] Mechnou, I.; Mourtah, I.; Raji, Y.; Chérif, A.; Lebrun, L.; Hlaibi, M.,Effective Treatment and the Valorization of Solid and Liquid Toxic Discharges from Olive Oil Industries, for Sustainable and Clean Production of Bio-Coal. *J. Clean. Prod*., **2021**, *288*, DOI: 10.1016/ j.jclepro.2020.125649.

[16] Soni, A.; Das, P. K.; Yusuf, M.; Kamyab, H.; Chelliapan, S., Development of Sand-Plastic Composites as Floor Tiles Using Silica Sand and Recycled Thermoplastics: A Sustainable Approach for Cleaner Production., *Sci. Rep.,* **2022**, *12*, 1-19, DOI: 10.1038/s41598-022-19635-1.

[17] Moussout, H.; Ahlafi, H.; Aazza, M.; Chfaira, R.; Mounir, C., Interfacial Electrochemical Properties of Natural Moroccan Ghassoul (Stevensite) Clay in Aqueous Suspension. *Heliyon*., **2020**, *6*, DOI: 10.1016/j.heliyon. 2020.e03634.

[18] Pavlidou, S.; Papaspyrides, C. D., A Review on Polymer-Layered Silicate Nanocomposites. *Prog. Polym. Sci*., **2008**, *33*, 1119-1198, DOI: 10.1016/ j.progpolymsci.2008.07.008.

[19] Jeong, G. Y.; Park, M. Y.; Kandler, K.; Nousiainen, T.; Kemppinen, O., Mineralogical Properties and Internal Structures of Individual Fine Particles of Saharan Dust. *Atmos. Chem. Phys.,* **2016**, *16*, 12397-12410, DOI: 10.5194/acp-16-12397-2016.

[20] Rhouta, B.; Kaddami, H.; Elbarqy, J.; Amjoud, M.; Daoudi, L.; Maury, F.; Senocq, F.; Maazouz, A.; Gerard, J. -F., Elucidating the Crystal-Chemistry of JbelRhassoulStevensite (Morocco) by Advanced Analytical Techniques. *Clay Miner*., **2008**, *43*, 393-403, DOI :10.1180/claymin.2008.043.3.05.

[21] Bejjaoui, R.; Benhammou, A.; Nibou, L.; Tanouti, B.; Bonnet, J. P.; Yaacoubi, A.; Ammar, A., Synthesis and Characterization of Cordierite Ceramic from Moroccan Stevensite and Andalusite. *Appl. Clay Sci*., **2010**, *49*, 336-340, DOI: 10.1016/j.clay.2010.06.004.

[22] Tokarský, J., Ghassoul – Moroccan Clay with Excellent Adsorption Properties. *Mater. Today, Proc*., **2018**, *5*, S78–S87, DOI: 10.1016/j.matpr.2018.05.060.

[23] Naboulsi, A.; Himri, M. El; Gharibi, E. K.; Haddad, M., El Study of Adsorption Mechanism of Malachite Green (MG) and Basic Yellow 28 (BY28) onto Smectite Rich Natural Clays (Ghassoul) Using DFT/B3LYP and DOE/FFD. *Surfaces and Interfaces*., **2022**, *33*, 102227, DOI: 10.1016/j.surfin.2022.102227.

[24] Bouna, L.; Rhouta, B.; Amjoud, M.; Jada, A.; Maury, F.; Daoudi, L.; Senocq, F., Correlation between Eletrokinetic Mobility and Ionic Dyes Adsorption of Moroccan Stevensite. *Appl. Clay Sci*., **2010**, *48*, 527-530, DOI: 10.1016/j.clay.2010.02.004.

[25] Brito, D. F.; Da Silva Filho, E. C.; Fonseca, M. G.; Jaber, M., Organophilic Bentonites Obtained by Microwave Heating as Adsorbents for Anionic Dyes. *J. Environ. Chem. Eng*., **2018**, *6*, 7080-7090, DOI: 10.1016/ j.jece.2018.11.006.

[26] Aloulou, W.; Hamza, W.; Aloulou, H.; Oun, A.; Khemakhem, S.; Jada, A.; Chakraborty, S.; Curcio, S.; Amar, R., Ben Developing of Titania-Smectite Nanocomposites UF Membrane over Zeolite Based Ceramic Support. *Appl. Clay Sci*., **2018**, *155*, 20-29, DOI: 10.1016/j.clay.2017.12.035.

[27] Lagaly, G.; Ogawa, M.; Dékány, I., Chapter 7.3 Clay Mineral Organic Interactions. *Dev. Clay Sci.,* **2006**, *1*, 309-377, DOI: 10.1016/S1572-4352(05)01010-X.

[28] Delavernhe, L.; Pilavtepe, M.; Emmerich, K., Cation Exchange Capacity of Natural and Synthetic Hectorite. *Appl. Clay Sci*., **2018**, *151*, 175-180,

DOI: 10.1016/j.clay.2017.10.007.

[29] Cruz-Guzmán, M.; Celis, R.; Hermosín, M. C.; Koskinen, W. C.; Nater, E. A.; Cornejo, J., Heavy Metal Adsorption by Montmorillonites Modified with Natural Organic Cations. *Soil Sci. Soc. Am. J.*, **2006**, *70*, 215-221, DOI: 10.2136/sssaj2005.0131.

[30] Al Bsoul, A.; Hailat, M.; Abdelhay, A.; Tawalbeh, M.; Al-Othman, A.; Al-kharabsheh, I. N.; Al-Taani, A. A., Efficient Removal of Phenol Compounds from Water Environment Using Ziziphus Leaves Adsorbent., *Sci. Total Environ.*, **2021**, *761*, 143229, DOI: 10.1016/j.scitotenv.2020.143229.

[31] Ghemit, R.; Makhloufi, A.; Djebri, N.; Flilissa, A.; Zerroual, L.; Boutahala, M., Adsorptive Removal of Diclofenac and Ibuprofen from Aqueous Solution by Organobentonites: Study in Single and Binary Systems. *Groundw. Sustain. Dev*., **2019**, *8*, 520-529, DOI: 10.1016/j.gsd.2019.02.004.

[32] Wakkel, M.; Khiari, B.; Zagrouba, F., Textile Wastewater Treatment by Agro-Industrial Waste: Equilibrium Modelling, Thermodynamics and Mass Transfer Mechanisms of Cationic Dyes Adsorption onto Low-Cost Lignocellulosic Adsorbent. *J. Taiwan Inst. Chem. Eng.*, **2019**, *96*, 439-452, DOI: 10.1016/j.jtice.2018.12.014.

[33] Shams Jalbani, N.; Solangi, A. R.; Memon, S.; Junejo, R.; Ali Bhatti, A.; Lütfi Yola, M.; Tawalbeh, M.; Karimi-Maleh, H., Synthesis of New Functionalized Calix[4]Arene Modified Silica Resin for the Adsorption of Metal Ions: Equilibrium, Thermodynamic and Kinetic Modeling Studies., *J. Mol. Liq.*, **2021**, *339*, 116741, DOI: 10.1016/j.molliq.2021.116741.

[34] Ume, O. L.; Ekeoma, B. C.; Yusuf, M.; Al-Kahtani, A. A.; Ubaidullah, M.; Sillanpää, M., Batch Studies of Hexavalent Chromium Biosorption from Mining Wastewater Using Aspergillus Niger., *Results Chem.,* **2022**, *4*, DOI: 10.1016/j.rechem.2022.100490.

[35] Ajbary, M.; Santos, A.; Morales-Flórez, V.; Esquivias, L., Removal of Basic Yellow Cationic Dye by an Aqueous Dispersion of Moroccan Stevensite. *Appl. Clay Sci*., **2013**, *80-81*, 46-51, DOI: 10.1016/j.clay.2013.05.011.

[36] Allaoui, S.; Naciri Bennani, M.; Ziyat, H.; Qabaqous, O.; Tijani, N.; Ittobane, N.; Yu, L., Kinetic Study of the Adsorption of Polyphenols from Olive Mill Wastewater onto Natural Clay: Ghassoul. *J. Chem.*, **2020**, 2020, DOI: 10.1155/2020/7293189.

[37] Ziyat, H.; Naciri Bennani, M.; Hajjaj, H.; Qabaqous, O.; Arhzaf, S.; Mekdad, S.; Allaoui, S.; Xing, Y., Adsorption of Thymol onto Natural Clays of Morocco: Kinetic and Isotherm Studies. *J. Chem*., **2020**, 2020, DOI: 10.1155/2020/4926809.

[38] Elass, K.; Laachach, A.; Alaoui, A.; Azzi, M., Removal of Methyl Violet from Aqueous Solution Using a Stevensite-Rich Clay from Morocco. *Appl. Clay Sci*., **2011**, *54*, 90-96, DOI: 10.1016/j.clay.2011.07.019.

[39] Soni, A.; Yusuf, M.; Mishra, V. K.; Beg, M., An Assessment of Thermal Impact on Chemical Characteristics of Edible Oils by Using FTIR Spectroscopy., *Mater. Today Proc.,* **2022**, *68*, 710-716, DOI: 10.1016/j.matpr.2022.05.568.

[40] Salerno, P.; Asenjo, M. B.; Mendioroz, S., Influence of Preparation Method on Thermal Stability and Acidity of Al-PILCs. *Thermochim. Acta*., **2001**, *379*, 101-109, DOI: 10.1016/S0040-6031(01)00608-6.

[41] Msadok, I.; Hamdi, N.; Gammoudi, S.; Rodríguez, M. A.; Srasra, E., Effect of Cationic Surfactant HDPy + on the Acidity and Hydrophilicity of Tunisian Clay. Mater. *Chem. Phys*., **2019**, *225*, 279-283, DOI: 10.1016/j.matchemphys.2018.12.098.

[42] Kang, J.; Li, J.; Ma, C.; Yi, L.; Gu, T.; Wang, J.; Liu, S., Goethite/Montmorillonite Adsorption Coupled with Electrocoagulation for Improving Fluoride Removal from Aqueous Solutions. *RSC Adv.*, **2022**, *12*, 7475-7484, DOI: 10.1039/d1ra08503d.

[43] Kadri, Z.; Mechnou, I.; Zyade, S., Migration of Bisphenol A from Epoxy Coating to Foodstuffs. *Mater. Today Proc*., **2021**, *45*, 7584-7587, DOI: 10.1016/j.matpr.2021.02.581.

[44] Zhu, J.; Shen, W.; Ma, Y.; Ma, L.; Zhou, Q.; Yuan, P.; Liu, D.; He, H., The Influence of Alkyl Chain Length on Surfactant Distribution within Organo-Montmorillonites and Their Thermal Stability. *J. Therm. Anal. Calorim*., **2012**, *109*, 301-309, DOI: 10.1007/s10973-011-1761-9.

[45] Bentahar, Y.; Hurel, C.; Draoui, K.; Khairoun, S.; Marmier, N., Adsorptive Properties of Moroccan Clays for the Removal of Arsenic(V) from Aqueous Solution.

Appl. Clay Sci., **2016**, *119*, 385-392, DOI: 10.1016/j.clay.2015.11.008.

[46] Kabilaphat, J.; Khaorapapong, N.; Ontam, A.; Ogawa, M., Formation of Cadmium Sulfide and Zinc Sulfide Mixture in the Interlayer Space of Montmorillonite. *Eur. J. Inorg. Chem*., **2015**, *2015*, 1631-1637, DOI: 10.1002/ejic.201403164.Özcan

[47] Özcan, A. S.; Erdem, B.; Özcan, A., Adsorption of Acid Blue 193 from Aqueous Solutions onto Na-Bentonite and DTMA-Bentonite. J. *Colloid Interface Sci*., **2004**, *280*, 44-54, DOI: 10.1016/j.jcis.2004.07.035.

[48] Eren, Z.; Acar, F. N., Adsorption of Reactive Black 5 from an Aqueous Solution: Equilibrium and Kinetic Studies. *Desalination*., **2006**, *194*, 1-10, DOI: 10.1016/j.desal.2005.10.022.

[49] Bulut, Y.; Aydin, H., A Kinetics and Thermodynamics Study of Methylene Blue Adsorption on Wheat Shells. *Desalination*., **2006**, *194*, 259-267, DOI: 10.1016/j.desal.2005.10.032.

[50] Gilchrist, G. F. R.; Gamble, D. S.; Kodama, H.; Khan, S. U., Atrazine Interactions with Clay Minerals: Kinetics and Equilibria of Sorption. *J. Agric. Food Chem*., 1**993**, *41*, 1748-1755, DOI: 10.1021/jf00034a043.

[51] Pignatello, J. J.; Xing, B., Mechanisms of Slow Sorption of Organic Chemicals to Natural Particles. *Environ. Sci. Technol*., **1996**, *30*, 1-11, DOI: 10.1021/es940683g.

[52] Nicholls, P. H., Factors Influencing Entry of Pesticides into Soil Water., *Pestic. Sci*., **1988**, *22*, 123-137, DOI: 10.1002/ps.2780220204.

[53] Dominguez, C. M.; Romero, A.; Lorenzo, D.; Santos, A., Thermally Activated Persulfate for the Chemical Oxidation of Chlorinated Organic Compounds in Groundwater. *J. Environ. Manage.,* **2020**, *261*, 110240, DOI: 10.1016/j.jenvman.2020.110240.

[54] Crini, G.; Peindy, H. N.; Gimbert, F.; Robert, C., Removal of C.I. Basic Green 4 (Malachite Green) from Aqueous Solutions by Adsorption Using Cyclodextrin-Based Adsorbent: Kinetic and Equilibrium Studies. *Sep. Purif. Technol*., **2007**, *53*, 97-110, DOI: 10.1016/j.seppur.2006.06.018.

[55] Azizian, S.; Haerifar, M.; Bashiri, H., Adsorption of Methyl Violet onto Granular Activated Carbon: Equilibrium, Kinetics and Modeling. *Chem. Eng. J*., **2009**, *146*, 36-41, DOI: 10.1016/j.cej.2008.05.024.

[56] Dubey, S. P.; Gopal, K., Application of Natural Adsorbent from Silver Impregnated Arachis Hypogaea Based Thereon in the Processes of Hexavalent Chromium for the Purification of Water. *J. Hazard. Mater*., **2009**, *164*, 968-975, DOI: 10.1016/j.jhazmat.2008.08.111.

[57] Sari, A.; Tuzen, M., Kinetic and Equilibrium Studies of Biosorption of Pb(II) and Cd(II) from Aqueous Solution by Macrofungus (Amanita Rubescens) Biomass. *J. Hazard. Mater*., **2009**, *164*, 1004-1011, DOI: 10.1016/j.jhazmat.2008.09.002.

[58] Ada, K.; Ergene, A.; Tan, S.; Yalçin, E., Adsorption of Remazol Brilliant Blue R Using ZnO Fine Powder: Equilibrium, Kinetic and Thermodynamic Modeling Studies*. J. Hazard. Mater*., **2009**, *165*, 637-644, DOI: 10.1016/j.jhazmat.2008.10.036.

[59] Mechnou, I.; Meskini, S.; El Ayar, D.; Lebrun, L.; Hlaibi, M., Olive Mill Wastewater from a Liquid Biological Waste to a Carbon/Oxocalcium Composite for Selective and Efficient Removal of Methylene Blue and Paracetamol from Aqueous Solution. *Bioresour. Technol.,* **2022**, *365*, 128162, DOI: 10.1016/j.biortech.2022.128162.

[60] Kausar, A.; Iqbal, M.; Javed, A.; Aftab, K.; Nazli, Z. I. H.; Bhatti, H. N.; Nouren, S., Dyes Adsorption Using Clay, and Modified Clay: A Review. *J. Mol. Liq*., **2018**, *256*, 395-407, DOI: 10.1016/j.molliq.2018.02.034.

[61] Özcan, A.; Ömeroğlu, Ç.; Erdoğan, Y.; Özcan, A. S., Modification of Bentonite with a Cationic Surfactant: An Adsorption Study of Textile Dye Reactive Blue 19. *J. Hazard. Mater*., **2007**, *140*, 173-179, DOI: 10.1016/j.jhazmat.2006.06.138.

[62] Gök, Ö.; Özcan, A. S.; Özcan, A., Adsorption Behavior of a Textile Dye of Reactive Blue 19 from Aqueous Solutions onto Modified Bentonite. *Appl. Surf. Sci*., **2010**, *256*, 5439-5443, DOI: 10.1016/j.apsusc.2009.12.134.

[63] Monsef Khoshhesab, Z.; Ahmadi, M., Removal of Reactive Blue 19 from Aqueous Solutions Using NiO Nanoparticles: Equilibrium and Kinetic Studies*. Desalin. Water Treat*., **2016**, *57*, 20037-20048, DOI: 10.1080/19443994.2015.1101713.

[64] Moussavi, G.; Mahmoudi, M., Removal of Azo and

Anthraquinone Reactive Dyes from Industrial Wastewaters Using MgO Nanoparticles. *J. Hazard. Mater*. **2009**, *168*, 806-812, DOI: 10.1016/j.jhazmat.2009.02.097.

[65] Auta, M.; Hameed, B. H., Optimized and Functionalized Paper Sludge Activated with Potassium Fluoride for Single and Binary Adsorption of Reactive Dyes. *J. Ind. Eng. Chem*., **2014**, *20*, 830-840, DOI: 10.1016/j.jiec.2013.06.013.

[66] Xue, Y.; Hou, H.; Zhu, S., Adsorption Removal of Reactive Dyes from Aqueous Solution by Modified Basic Oxygen Furnace Slag: Isotherm and Kinetic Study. *Chem. Eng. J.*, **2009**, *147*, 272-279, DOI: 10.1016/j.cej.2008.07.017.

[67] Moslemizadeh, A.; Khezerloo-ye Aghdam, S.; Shahbazi, K.; Khezerloo-ye Aghdam, H.; Alboghobeish, F., Assessment of Swelling Inhibitive Effect of CTAB Adsorption on Montmorillonite in Aqueous Phase. *Appl. Clay Sci*., **2016**, *127-128*, 111-122, DOI: 10.1016/j.clay.2016.04.014.